Functional Materials 17, No.2 (2010)

Molecular dynamics of graphene preparation by mechanical exfoliation of a graphite surface

A.V.Khomenko, N.V.Prodanov

Sumy State University, 2 Rimsky-Korsakov St., 40007 Sumy, Ukraine

Received October 12, 2009

Classical molecular dynamics has been used to investigate physical processes occurring when a rigid adhesive nanobump of a crystalline surface is approached to and lifted from a graphite sample. Nanobumps with two different lattice constants are considered. The behavior of the system is studied under conditions of several interaction values between the two interfacing materials and the nanobump movement. Values of the bump-sample interaction energies sufficient for micromechanical cleavage of a graphite surface, resulting in the formation of a graphene layer attached to the nanobump are determined.

Классическая молекулярная динамика использована для исследования физических процессов, имеющих место при приближении к графитовому образцу и отводе от него жесткого адгезивного нановыступа кристаллической поверхности. Рассмотрены нановыступы с двумя различными постоянными решетки. Поведение системы изучено в условиях нескольких значений величины взаимодействия смежных материалов и скорости движения нановыступа. Определены энергии взаимодействия выступ — образец, достаточные для микромеханического раскалывания поверхности графита, в результате которого образуется слой графена, прикрепленный к нановыступу.

1. Introduction

Graphene is a single layer of carbon atoms densely packed in a honeycomb crystal lattice [1-3]. Graphene may exhibit unusual electronic behavior. For example, charge carriers in graphene behave as massless Dirac fermions [4], and such phenomena as the inacceptability of the Born-Oppenheimer approximation [5] and a room-temperature quantum Hall effect [6] have been observed. Graphene exhibits simultaneously high plasticity (folds and bends are commonly observed) and brittleness (it fractures like glass at high strains).

Recently, significant progress was achieved in developing the methods of ultrasonic cleavage of graphite [8] and some epitaxial growth techniques [7]. However, the full growing cycle of a single-layer graphene has not yet been demonstrated. The standard procedure of graphene preparation is the micromechanical cleavage [1–3], that allows splitting this strongly layered material into individual atomic planes.

Micromechanical cleavage or exfoliation technique has been studied mainly in experiment. Exfoliation of graphite plays an important role in nanotribology, where the superlubricity phenomenon is mainly attributed to the cleavage of graphite surface, resulting in a small flake attached to the tip of a friction force microscope (FFM) [9]. Theoretical confirmation of the flake cleavage and the determination of its formation conditions can of practical interest [10, 11].

The mentioned facts have spurred computer experiments described in this paper. The model of a crystalline nanobump interacting with a graphite sample is studied using classical molecular dynamics (MD). The considered system mimics graphene preparation by micromechanical cleavage and the experiments concerning the superlubricity. The nanobump can be considered as a part of the scotch tape surface used for graphite peeling or as a nanobump of a FFM

tip. The nanobump movement process can be considered as the nanoindentation of the graphite surface, as it may happen in the experiments where the FFM tip is involved. The main aims of the simulations are to investigate the influence of the nanobump lattice constant, the magnitude of the tip-sample interaction and the nanoindentation rate on the system behavior and to define the conditions favorable for graphite exfoliation and the formation of a graphene flake.

2. Methodology

The graphitic sample consists of three graphene layers with AB stacking which reflects α form of graphite (Fig. 1). The armchair and zigzag graphene edges lie along x and y coordinates axes, respectively, and periodical boundary conditions are applied in the xy plane. Each layer is composed of 24×24 honeycombs, thus containing 3456 carbon atoms and the lengths along x and y directions are 10.082 nm and 8.731 nm, respectively. To hold the sample in place, the bottom graphitic layer remains rigid during the simulations.

The graphite surface interacts with an absolutely rigid square pyramidal nanobump (which will be also referred to as the tip). Although in real experiments materials have finite stiffness, the absolutely rigid surfaces are often used in MD experiments [12–18] and such an approximation is applied to the nanobump in the present study. The bump consists of five layers of atoms parallel to the xy plane and particles are arranged in a perfect bcc lattice. Two values of lattice constant a equal to 0.3165 nm and 0.1583 nm are considered, where the former value corresponds to the crystal structure of tungsten [19] which is used in experiments with FFM. The tapered shape is provided by adding one atomic row in x and y directions per layer when moving from the tip bottom to its top. The bottom atomic layer exposes (001) crystallographic plane and contains 13×13 atoms. The nanobump contains 1135 atoms and the total number of particles involved in the simulations is 11503. We consider two values of a to investigate the influence of the surface energy and tip dimensions on the system behavior.

The Brenner potential [14, 20–22] is used for covalent bonds between carbon atoms within the two upper dynamic graphene layers. It has the form:

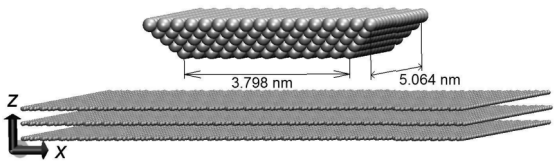

Fig.1. Perspective view of the initial atomic configuration of the system for a=0.3165nm (all snapshots in this work are produced using Visual Molecular Dynamics software [12]).

$$V_B = \sum_i \sum_{j>i} [V^R(r_{ij}) - b_{ij} V^A(r_{ij})]. \quad (1)$$

In this study, expressions of a second-generation reactive empirical bond order (REBO) form of the potential [21] are used for pair-additive interactions $V^R(r_{ij})$ and $V^A(r_{ij})$. They are defined as follows:

$$V^R(r) = f^c(r)(1 + Q/r)Ae^{-\alpha r}, \quad (2)$$

$$V^A(r) = f^c(r)\sum_{n=1}^{3} B_n e^{-\beta_n r}. \quad (3)$$

Here $B_1 = 12388.792$ eV, $\beta_1 = 4.721$ Å^{-1}, $Q = 0.314$ Å, $B_2 = 17.567$ eV, $\beta_2 = 1.433$ Å^{-1}, $A = 10953.544$ eV, $B_3 = 30.715$ eV, $\beta_3 = 1.383$ Å^{-1}, $\alpha = 4.747$ Å^{-1}, $D_{min} = 1.7$ Å, $D_{max} = 2.0$ Å. The function $f^c(r)$ in (2) and (3) limits the range of the covalent interactions and has the form:

$$f^c(r) = \begin{cases} 1, & r < R_{ij}^{(1)}, \\ \left[1 + \cos\left[\dfrac{\pi(r - R_{ij}^{(1)})}{(R_{ij}^{(2)} - R_{ij}^{(1)})}\right]\right]/2, & R_{ij}^{(1)} < r < R_{ij}^{(2)}, \\ 0, & r > R_{ij}^{(2)}, \end{cases} \quad (4)$$

where $R_{ij}^{(1)} = D_{min}$ and $R_{ij}^{(2)} = D_{max}$ are cutoff distances.

The bond order function b_{ij} in (1) is chosen as in the first version of Brenner potential with parameters for potential II in [20]. The chosen simplified potential form implies that we do not intend to accurately simulate the in-plane behavior of graphene layers. The interactions from Brenner potential are computed using parallel algorithm presented in [22].

For realistic modeling of processes related to graphite cleavage, the crucial role may play the proper description of the interactions between graphene layers [23, 24]. In this work, we use registry-dependent inter-

layer potential (RDP) that can describe the potential relief in graphitic systems at a reasonable accuracy [24]. It is defined as follows:

$$V(\mathbf{r}_{ij},\mathbf{n}_i,\mathbf{n}_j) = \tag{5}$$
$$= e^{-\lambda(r_{ij}-z_0)}\left[C + f(\rho_{ij}) + f(\rho_{ji})\right] - A\left(\frac{r_{ij}}{z_0}\right)^{-6}.$$

Here $\lambda = 3.629$ Å^{-1}, $z_0 = 3.34$ Å, $C = 3.030$ meV, $A = 10.238$ meV. The potential contains r^{-6} van der Waals (vdW) attraction and an exponentially decaying repulsion due to the interlayer wavefunction overlap. To reflect the overlap anisotropy, the function f is introduced which rapidly decays with the transverse distance ρ:

$$f(\rho) = e^{-(\rho/\delta)^2}\sum C_{2n}(\rho/\delta)^{2n}, \tag{6}$$

where $C_0 = 15.71$ meV, $C_2 = 12.29$ meV, $C_4 = 4.933$ meV and ρ is defined via the distance r_{ij} between pairs of atoms i and j belonging to distinct layers and the vector $\mathbf{n}_k$ ($k = i,j$) which is normal to the sp^2 plane in the vicinity of atom k:

$$\rho_{ij} = r_{ij}^2 - (\mathbf{n}_i\mathbf{r}_{ij})^2,\ \rho_{ji} = r_{ij}^2 - (\mathbf{n}_j\mathbf{r}_{ij})^2. \tag{7}$$

In this study, $\mathbf{n}_k$ is computed as the "local" normal, i. e. as average of the three normalized cross products of the displacement vectors to the nearest neighbors of atom k, and this corresponds to RDP1 in [24]. For long-range vdW term, the cutoff distance is equal to $r_c = 2.7z_0 = 0.9018$ nm. The interlayer binding energy is calculated as

$$E_{il} = \sum_i \sum_{j>i} V(\mathbf{r}_{ij},\mathbf{n}_i,\mathbf{n}_j). \tag{8}$$

In (8), summation is performed over carbon atoms of the two adjacent layers and function V is defined using formula (5).

The presence of normals in the RDP makes it in essence a many-body potential which requires much more computational effort as compared to simple pairwise potentials. In this study, only interactions between the adjacent layers are considered and they are computed using a specially developed parallel algorithm based on linked cell lists [13, 14].

The tip is assumed to interact only with the upper graphitic layer and interactions between the tip and carbon atoms are described via Lennard-Jones (LJ) pairwise potential

$$V_{LJ} = 4\varepsilon\left[\left(\frac{\sigma}{r}\right)^{12} - \left(\frac{\sigma}{r}\right)^{6}\right],\ r < r_c,\ V_{LJ} = 0,\ r \ge r_c, \tag{9}$$

where r is the distance between a pair of atoms in interfacing materials, $\sigma = 0.5z_0$, and the cutoff distance r_c is the same as for the RDP1. As the true values of forces acting between the tip and the surface are not firmly established, we investigate the system behavior for several values of ε, namely, 0.1, 0.25, 0.5, 1, and 6 eV. The equations of motion are integrated using the leapfrog method [13] using the time step $\Delta t = 0.1$ fs. The heat is dissipated through the Berendsen thermostat coupled with two dynamic graphitic layers and implemented as in [14].

We will study two modes of the nanobump movement. The first is indentation which takes place when the tip is allowed to advance past the contact point and the sample is compressed by the nanobump. The second is contact which is observed when the tip is pulled toward the surface only up to contact, after which it is retracted from the sample. The indentation process proceeds as follows. After equilibration of the system during 1 ps with the tip outside the range of interaction hung at 1.16 nm and 1.08 nm above the surface for a equal to 0.3165 nm and 0.1583 nm, respectively, the bump is lowered towards the surface. The tip movement occurs by changing z coordinates of the tip atoms in increments of 0.01304 nm and 0.01182 nm for the larger and smaller a, respectively. Note that nanobump with $a = 0.3165$ nm does not reach the equilibrium position of the upper graphene layer and the smallest distance between proximal layers of the interfacing materials is about 0.108 nm. In contrast, smaller tip is lowered below the upper graphite layer by about 0.076 nm. After reaching the minimum distance, the tip is immediately pulled away from the surface. The entire system is equilibrated for 0.05 and 0.04 ps in between the nanobump displacements. The mentioned quantities correspond to the indentation speeds of 260.8 m/s and 295.5 m/s. When contact is considered, the tip is not immediately withdrawn from the surface but after reaching the minimum height of about 0.3 nm relatively to the upper graphene layer, it is hung for 0.2 ps in order to allow the formation of the contact between the surfaces. The contact mode is used mainly to investi-

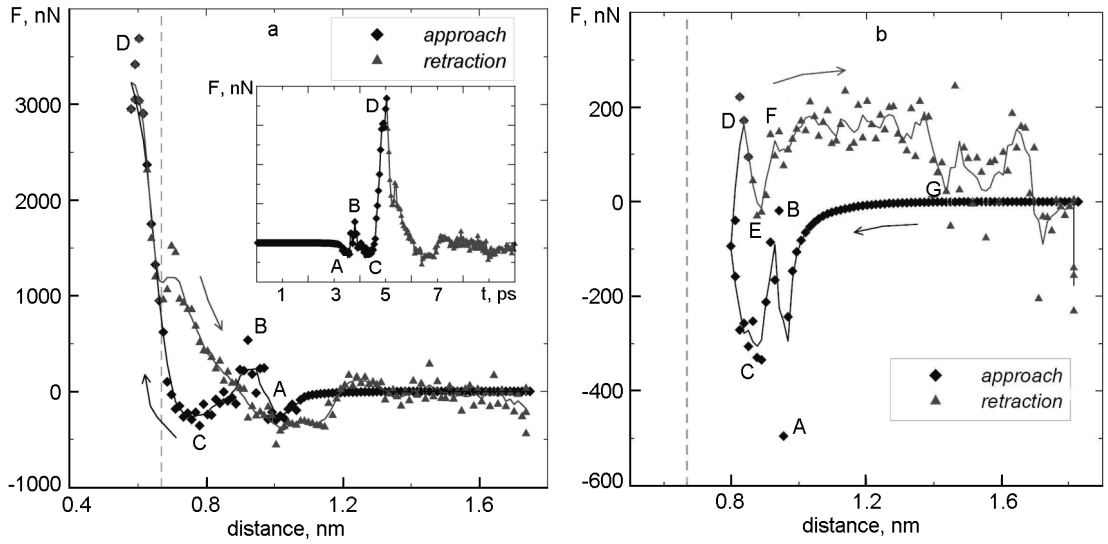

Fig. 2. Normal force acting on the nanobump as it indents in and then is withdrawn from the graphitic surface for $\varepsilon = 0.5$ eV and $a = 0.1583$ nm (a), $a = 0.3165$ nm (b). The abscissa values correspond to the vertical distance between the rigid graphene layer and the bottom atomic layer of the tip. Solid lines depict the weighted averages of measured data and are shown to guide the eye. Arrows indicate the direction of the nanobump movement. Dashed line presents the equilibrium position of the upper carbon layer which is assumed to be 0.668 nm from the bottom carbon layer. Inset in (a): time dependence of force F, time varies from 0 to 10 ps, ordinate values are the same as in the main figure.

gate the flake formation and much higher indentation speeds equal to 4814 m/s and 2880 m/s for larger and smaller tip are used in this case. The duration of simulations at low and high speed is 10 ps and 2.5 ps, respectively.

In experiments using force microscopy, force-versus-distance curves are obtained, which reflect the changes of the normal force acting on the tip as a function of the distance to the surface. In this work, this force F is computed as the sum of z components of forces acting on the nanobump atoms from the graphitic sample, and it is averaged over the last 0.01 ps of the equilibration procedure in between the tip displacements. The next section presents these curves and other results obtained in the simulations.

3. Results and discussion

During 1 ps after the equilibration period of the simulations when the forces between the tip and the sample are still zero, the average values of interlayer distance and the energy between the upper two dynamic graphene layers are about 0.336±0.004 nm and 41.6±0.8 meV, respectively. These values differ from 0.334 nm and 48 meV computed for rigid layers using RDP [24] by about 1 % and 15 %, respectively. The discrepancy may be attributed to the finite cutoff distance used in this study, thermal fluctuations of normals and the use of local normals instead of semilocal ones. Nevertheless, the obtained values are very close to the experimental ones [24].

The results obtained in simulations of indentation and contact will now be considered separately.

Indentation. Fig. 2a shows force-vs-distance curve and time dependence of the normal force F acting on the nanobump at $a = 0.1583$ nm. Following an initial slow variation of the force between the graphite substrate and the nanobump as the latter is being pulled toward the surface, the onset of an instability is observed, manifested as a sharp increase in the attraction between the two (point A in Fig. 2a). This corresponds to a jump-to-contact (JC) phenomenon [15, 25] which occurs as a fast process where carbon atoms under the bump are displaced toward it in a short time span of about 0.5 ps and it is associated primarily with a tip-induced sample deformation [15]. In Fig. 3a, one can note the consequence of JC as a small local maximum of the interlayer energy E_{il} for $\varepsilon = 1$ eV in between 3 and 4 ps. The JC results in collisions of carbon atoms with absolutely rigid nanobump and they cause a sharp peak in the force-displacement curve (point B in

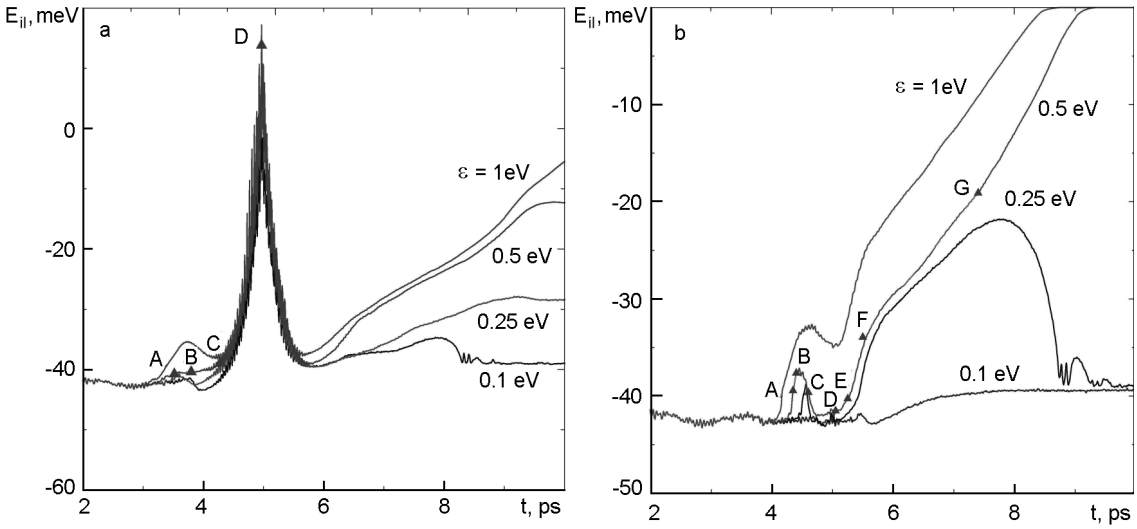

Fig. 3. Time dependences of the binding energy of the upper two graphite layers (after equilibration period) for different magnitudes of tip-sample interactions, a = 0.1583 nm (a) and a = 0.3165 nm (b).

Fig. 2a). The further advancement of the tip towards the sample results in the increase of attraction (*BC* segment of the curves), and after reaching the point *C*, a new dramatic increase of repulsion is observed suggesting the repulsive wall region and the indentation of the sample [15]. Video animation sequences of the simulations indicate that indentation results in a further sample deformation characterized by an adhesion-induced flow of carbon atoms which wet the tip edges. The relatively deep penetration of the nanobump used for $a = 0.1583$ nm results in sharp peaks at about 5 ps in Fig. 3a. Lifting the tip from the sample results in enhanced adhesion between the nanobump and the surface. This is evidenced by hysteresis in the force curves in Fig. 2a and also by the increase of the interlayer energy E_{il} in Fig. 3a, which suggests the separation of the graphene layers. However, the final height used in the present simulation is insufficient for complete exfoliation of the upper graphene layer as can be seen from Fig. 4a where the final atomic configuration of the system is shown.

The loading part of the force-displacement curve obtained during indentation of the sample with a larger nanobump (Fig. 2b) is qualitatively similar to the described above for the smaller tip. It indicates the presence of a JC (point *A* in Fig. 2b) which corresponds to local maxima of E_{il} observed in between 4 and 5 ps in Fig. 3b. There is also a sharp peak in point *B* and a repulsive wall region (segment *CD*). The withdrawal part of the force-displacement curve in Fig. 2b, however, is qualitatively different from that shown in Fig. 2a. A moderate decrease of repulsion during the initial retraction stage till point *E* is followed by the segment *EF* where the force becomes repulsive once more and it retains the positive sign till point *G* is reached. This exhibits the tendency of carbon atoms to push the tip upwards and hence to move in this direction, thus stimulating the exfoliation of the upper layer. A sudden change of repulsion to attraction after point *G* in Fig. 2b is indicative of the final stage of exfoliation, where forces between graphene sheets at their boundaries should be overcome and the bending of the upper layer is observed. The ultimate configuration includes the completely removed upper layer (Fig. 4b) corresponding to zero interlayer energy in Fig. 3b.

Comparing the force-displacement curves for smaller and larger tips, one can note that data scattering is much more manifested in the latter case. This may be ascribed to the larger surface area of the nanobump with $a = 0.3165$ nm and its lower surface energy which provide the conditions for greater number of irregular atomic collisions with the tip due to thermal motion of carbon atoms. In some works, the force-displacement curves are averaged additionally to filter out the noise from thermal vibrations [26, 27]. This procedure has not been carried out in this study.

The influence of the tip-sample interaction magnitude ε on the system behavior can be concluded from Fig. 3. For $a = 0.1583$ nm, the time dependences of E_{il} during retrac-

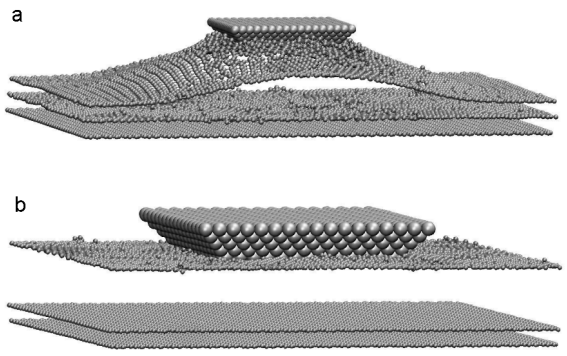

Fig. 4. System at the end of the simulation of indentation with ε = 0.5 eV, a = 0.1583 nm (a) and a = 0.3165 nm (b).

tion (which begins after 5 ps) exhibit a slow increase for all ε except 0.1 eV (Fig. 3a). The larger ε cause larger E_{il} indicating a higher trend to exfoliation with increase in ε. The complete exfoliation, however, was not observed for the smaller tip due to a rather small ultimate distance between the nanobump and the sample. For ε = 0.1 eV in Fig. 3a, there is a small local maximum at about 8 ps after which E_{il} has almost constant value. This suggests that the nanobump "losses" the upper graphene layer and carbon atoms return to the equilibrium vertical position of the upper layer. For a = 0.3165 nm, it is to note the absence of a sharp peak at about 5 ps for all ε in Fig. 3b due to shallow indentation. In this case, there is no significant adhesion for ε = 0.1 eV, when at ε = 0.25 eV, the tip "losses" carbon atoms and ε values of 0.5 eV and larger cause the complete exfoliation of the upper graphene layer.

Contact. In order to explore the formation possibility of a flake attached to the nanobump, second series of simulations has been carried out where contact has been considered. In these computer experiments, the tip is moved at high speeds and is not allowed to compress the substrate, but after the contact formation the bump is immediately pulled away from the sample. Significantly higher speeds as compared with the indentation are required to provide the conditions where the excess heat has not enough time to dissipate. This helps to reach high temperature values sufficient to contribute to breaking of covalent bonds in a graphene sheet. As the simulations show, greater values of ε are required for the flake formation. We consider the ε = 6 eV value and the case of a = 0.1583 nm. For

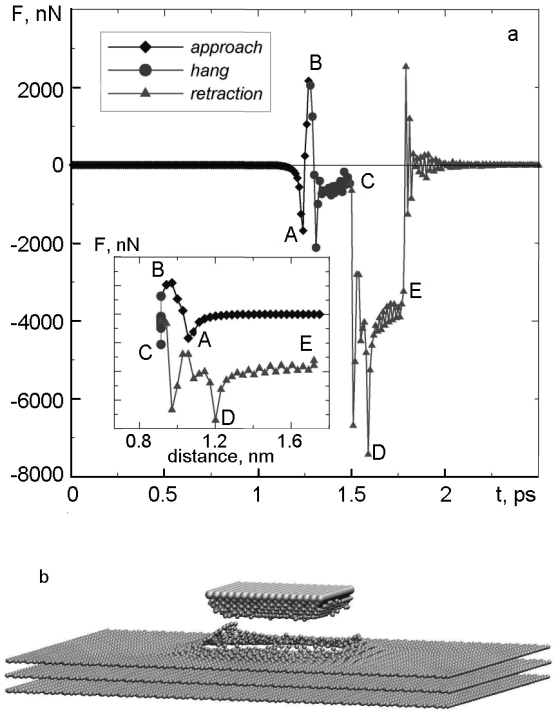

Fig. 5. (a) Time dependences of the normal force F acting on the nanobump with a = 0.1583 nm in the simulation concerning its contact with the graphite surface. Inset: force-displacement curve for this case, distance is computed as in Fig. 2, ordinate values are the same as in the main figure, the minimum abscissa value coincides with the equilibrium position of the upper graphene layer and the maximum abscissa value is 1.8 nm. (b) Snapshot of the system corresponding to point E in (a).

larger tip, the results are qualitatively similar. Note only that for a = 0.3165 nm, about double movement speeds are required than for the smaller tip.

When the tip is pulled toward the surface, a gradual increase of the attraction between the surfaces is observed, which is followed by a jump-to-contact (point A in Fig. 5a). A sudden jump in force is represented by segment AB, similar to the indentation case. The tip is hung in segment BC in order to achieve enough bonding between the surfaces. The retraction begins after point C and causes a sharp increase of attraction, with maximum in point D, after which it begins to decay and suddenly is switched to repulsion after point E. As animated video shows, the decrease in attraction is caused by rupture of interatomic bonds in the upper graphene layer. The breaking of the majority of bonds causes the formation of a flake, manifested as a considerable force change after point E. The

system atomic configuration at this point is shown in Fig. 5b, where the flake attached to the tip can be observed. The flake is very deformed and has almost completely lost its honeycomb lattice. The results obtained give reason to conclude that it is unlikely to experimentally observe the considered scenario of flake formation which occurs relatively far away from the graphene edges, because it requires very high indentation rates and surface energies of the tip. More probable is the cleavage occurring at a grain boundary of a polycrystalline graphite sample, which is used in the experiments [9], where the flake can be cleaved through the exfoliation mechanism considered in the previous subsection for larger tip.

4. Conclusions

Physical processes occurring during interaction of a graphite sample with a rigid pyramidal nanobump have been studied using classical molecular dynamics. Two values of the nanobump lattice constant a, 0.3165 nm and 0.1583 nm, have been considered under conditions of several magnitudes of tip-sample interaction and the nanoindentation speed. The simulations reveal what follows with regard to adhesion and exfoliation of graphite surface. The contact formation between a rigid tip approaching a soft graphitic substrate is associated with an atomic scale instability which results in the JC phenomenon. Separation of the two materials results in adhesion-induced wetting of the tip with carbon atoms for higher values of ε. It is imaged in the force-vs-distance curves which exhibit a pronounced hysteresis upon tip-to-sample approach and subsequent separation. Such wetting, however, is not observed for larger tip when $\varepsilon = 0.1$ eV. The nanobump "losses" the graphene layer when $\varepsilon = 0.1$ eV and $\varepsilon = 0.25$ eV for smaller and larger nanobump, respectively. Values of ε equal to or greater than 0.5 eV are sufficient for micromechanical cleavage of the sample when the nanobump with $a = 0.3165$ nm is considered. For the formation of a flake attached to the tip, considerably higher indentation speeds are required exceeding almost twice those for the larger nanobump.

Acknowledgements. We acknowledge the use of a Windows beowulf cluster at Informatics department of Sumy State University. The work has been done under financial support of the Fundamental Researches State Foundation of Ukraine (Grants F25/97-2008, F28/443-2009).

References

1. A.K.Geim, K.S.Novoselov, *Nature Mater.*, **6**, 183 (2007).
2. A.H.Castro Neto, F.Guinea, N.M.R.Peres et al., *Rev. Mod. Phys.*, **81**, 109 (2009).
3. K.S.Novoselov, A.K.Geim, S.V.Morozov et al., *Science*, **306**, 666 (2004).
4. K.S.Novoselov, A.K.Geim, S.V.Morozov et al., *Nature*, **438**, 197 (2005).
5. S.Pisana, M.Lazzeri, C.Casiraghi et al., *Nature Mater.*, **6**, 198 (2007).
6. K.S.Novoselov, Z.Jiang, Y.Zhang et al., *Science*, **315**, 1379 (2007).
7. A.K.Geim, *Science*, **324**, 1530 (2009).
8. Y.Hernandez, V.Nicolosi, M.Lotya et al., *Nature Nanotechnol.*, **3**, 563 (2008).
9. M.Dienwiebel, G.S.Verhoeven, N.Pradeep et al., *Phys. Rev. Lett.*, **92**, 126101 (2004).
10. G.S.Verhoeven, M.Dienwiebel, J.W.M.Frenken, *Phys. Rev.*, **B70**, 165418 (2004).
11. A.E.Filippov, M.Dienwiebel, J.W.M.Frenken et al., *Phys. Rev. Lett.*, **100**, 046102 (2008).
12. W.Humphrey, A.Dalke, K.Schulten, *J. Molec. Graphics*, **14**, 33 (1996).
13. D.C.Rapaport, The Art of Molecular Dynamics Simulation, 2nd ed., Cambridge University Press, Cambridge (2004).
14. M.Griebel, S.Knapek, G.Zumbusch, Numerical Simulation in Molecular Dynamics, Springer, Berlin, Heidelberg (2007).
15. S.J.Heo, S.B.Sinnott, D.W.Brenner, J.A.Harrison, in: B.Bhushan (Ed.), Nanotribology and Nanomechanics, Springer, Berlin (2005), p.623.
16. A.V.Khomenko, N.V.Prodanov, *Condens. Matter Phys.*, **11**, 615 (2008).
17. A.V.Khomenko, N.V.Prodanov, *High Press. Phys. and Techn.*, **19**, 123 (2009).
18. J.D.Schall, D.W.Brenner, *J. Mater. Res.*, **19**, 31729 (2004).
19. www.webelements.com
20. D.W.Brenner, *Phys. Rev.*, **B42**, 9458 (1990).
21. D.W.Brenner, O.A.Shenderova, J.A.Harrison et al., *J. Phys.:Condens. Matter*, **14**, 783 (2002).
22. A.Caglar, M.Griebel, in: R.Esser, P.Grassberger, J.Grotendorst, M.Lewerenz (Eds.), Molecular Dynamics on Parallel Computers, World Scientific, Julich (1999), p.1.
23. A.Ito, H.Nakamura, *Thin Solid Films*, **516**, 6553 (2008).
24. A.N.Kolmogorov, V.H.Crespi, *Phys. Rev.*, **B71**, 235415 (2005).
25. U.Landman, W.D.Luedtke, N.A.Burnham, R.J.Colton, *Science*, **248**, 454 (1990).
26. A.Garg, J.Han, S.B.Sinnott, *Phys. Rev. Lett.*, **81**, 2260 (1998).
27. A.Garg, S.B.Sinnott, *Phys. Rev.*, **B60**, 13786 (1999).

Молекулярна динаміка одержання графену механічним злущенням поверхні графіту

О.В.Хоменко, М.В.Проданов

Класичну молекулярну динаміку використано для дослідження фізичних процесів, які мають місце при наближенні до графітового зразка і відведенні від нього жорсткого адгезивного нановиступу кристалічної поверхні. Розглянуто нановиступи з двома різними значеннями сталої гратки. Поведінку системи вивчено в умовах декількох значень величини взаємодії суміжних матеріалів і швидкості руху нановиступу. Визначено енергії взаємодії виступ — зразок, достатні для мікромеханічного розколювання поверхні графіту, внаслідок якого утворюється шар графену, прикріплений до нановиступу.